

# A Bottom-Up Dynamic Model of Portfolio Credit Risk with Stochastic Intensities and Random Recoveries

Tomasz R. Bielecki<sup>1,\*</sup>, Areski Cousin<sup>2†</sup>,  
Stéphane Crépey<sup>3,‡</sup>, Alexander Herbertsson<sup>4,§</sup>

<sup>1</sup> Department of Applied Mathematics  
Illinois Institute of Technology  
Chicago, IL 60616, USA

<sup>2</sup> Université de Lyon,  
Université Lyon 1, Laboratoire SAF, EA 2429,  
Institut de Science Financière et d'Assurances,  
50 Avenue Tony Garnier, 69007 Lyon, France.

<sup>3</sup> Laboratoire Analyse et Probabilités  
Université d'Évry Val d'Essonne  
91037 Évry Cedex, France

<sup>4</sup> Centre for finance/Department of Economics  
University of Gothenburg  
SE 405 30 Göteborg, Sweden

August 26, 2013

---

\*The research of T.R. Bielecki was supported by NSF Grant DMS-0604789 and NSF Grant DMS-0908099.

†The research of A. Cousin benefited from the support of the DGE and the ANR project Ast&Risk.

‡The research of S. Crépey benefited from the support of the “Chaire Risque de Crédit” and of the “Chaire Marchés en Mutation”, Fédération Bancaire Française.

§The research of A. Herbertsson was supported by the Jan Wallander and Tom Hedelius Foundation and by Vinnova.

## Abstract

In [5], the authors introduced a Markov copula model of portfolio credit risk where pricing and hedging can be done in a sound theoretical and practical way. Further theoretical backgrounds and practical details are developed in [6] and [7] where numerical illustrations assumed deterministic intensities and constant recoveries. In the present paper, we show how to incorporate stochastic default intensities and random recoveries in the bottom-up modeling framework of [5] while preserving numerical tractability. These two features are of primary importance for applications like CVA computations on credit derivatives [10, 3, 2], as CVA is sensitive to the stochastic nature of credit spreads and random recoveries allow to achieve satisfactory calibration even for “badly behaved” data sets. This paper is thus a complement to [5], [6] and [7].

**Keywords:** Portfolio credit risk, Markov copula model, Common shocks, Stochastic spreads, Random recoveries.

**Acknowledgements:** We thank the anonymous referee for careful reading of the manuscript, for helpful comments, and for bringing to our attention important references.

## 1 Introduction

In [5, 6, 7] we introduced a common-shock Markov copula model of default times providing an effective joint calibration to single-name CDS and multi-name CDO tranches data. In this sense this model solves the portfolio credit risk top-down bottom-up puzzle [9]. For earlier, partial progress in this direction, see [17, 18, 19, 23] and the introductory discussion in [6]. The main model feature is the use of common jumps to default, triggered by common shocks, as a powerful dependence device also compatible with the Markov copula properties [12], the latter being required to decouple the calibration of the individual (single-name) model parameters from the model dependence parameters.

The model presented in [5] is a fully dynamic model in which the critical issue of modeling counterparty risk embedded in credit derivatives, and consequently the issue of computation and hedging of CVA, can be consistently and practically addressed [3, 8, 10, 15, 2]. However, it was emphasized in a June 2011 Bank of International Settlements press release that “During the financial crisis of 2007-09, roughly two-thirds of losses attributed to counterparty credit risk were due to CVA losses and only about one-third were due to actual defaults”. In other words, the volatility of CVA matters as much as its level. Consequently (and also to be consistent with the optional nature of the CVA), for CVA computations on credit derivatives, practitioners strongly advocate the use of stochastic default intensities. Moreover, in case of some “badly behaved” data sets, a satisfying calibration accuracy can only be achieved by resorting to random recoveries.

In order to respond to these considerations, in the present paper, which is a follow-up to [5, 6, 7], we provide more background, implementation hints, as well as numerical illustration accounting for these two features which are important for applications: stochastic spreads and random recoveries. Section 2 reviews the model of default times which is used, including the specification of the stochastic intensities and recoveries. Regarding the default intensities, we resort to time-inhomogenous affine processes with time-dependent piecewise-constant mean-reversion level, resulting in analytical tractability and calibration flexibility (of the term-structure of CDS spreads in particular). For tractability reasons, random recoveries are taken to be independent between them, as well as independent from everything else in the model. Section 3 is about pricing in this setup. In particular pricing of CDS, as well as of CDO tranches, ultimately boils down here to computations of Laplace transform for time-inhomogenous affine processes. Proposition 3.2 shows how this can be done explicitly, exploiting the piecewise-constant mean-reversion structure of the intensities. Again, effective joint calibration of this model to CDS and CDO data is an important achievement. Section 4 reviews in detail and illustrates the calibration methodology, regarding in particular the stochastic affine intensities and random recovery specifications which are used.

In the rest of the paper we consider a risk neutral pricing model  $(\Omega, \mathcal{F}, \mathbb{P})$ , for a filtration  $\mathcal{F} = (\mathcal{F}_t)_{t \in [0, T]}$  which will be specified below, and where  $T \geq 0$  is a fixed time horizon. We denote  $\mathbb{N}_n = \{1, \dots, n\}$  and we let  $\mathcal{N}_n$  denote the set of all subsets of  $\mathbb{N}_n$ , where  $n$  represents the number of obligors in the underlying credit portfolio. We also let  $\tau_i$  and  $H_t^i = \mathbb{1}_{\{\tau_i \leq t\}}$  denote the default time of name  $i = 1, 2, \dots, n$  and the corresponding indicator process.

## 2 Model of Default Times

We recall a common shocks portfolio credit risk model of [5, 6, 7]. In order to describe the defaults we define a certain number  $m$  (typically small: a few units) of groups  $I_j \subseteq \mathcal{N}_n$ , of obligors who are likely to default simultaneously, for  $j \in \mathbb{N}_m$ . More precisely, the idea is that at every time  $t$ , there will be a positive probability that the survivors of the group of obligors  $I_j$  (obligors of group  $I_j$  still alive at time  $t$ ) default simultaneously. Let  $\mathcal{I} = \{I_1, \dots, I_m\}$ ,  $\mathcal{Y} = \{\{1\}, \dots, \{n\}, I_1, \dots, I_m\}$ . Given non-negative constants  $a$ ,  $c$  and non-negative deterministic functions  $b_Y(t)$  for  $Y \in \mathcal{Y}$ , let a “shock intensity process”  $X^Y$  be defined in the form of an extended CIR process as:  $X_0^Y$  a given constant, and for  $t \in [0, T]$

$$dX_t^Y = a(b_Y(t) - X_t^Y) dt + c\sqrt{X_t^Y} dW_t^Y \quad (1)$$

where the Brownian motions  $W^Y$  are independent.

**Remark 2.1** We refer the reader to [10] for a preliminary version of this model dedicated to valuation and hedging of counterparty risk on a CDS. The use of extended CIR processes as drivers of default intensities is motivated by the following arguments.

- The numerical results of [10] illustrate that such extended CIR specifications of the intensities, with time dependent and piecewise constant functions  $b_Y(\cdot)$ ,<sup>1</sup> in addition to being compatible with the underlying Markov copula structure of a portfolio credit risk model, are appropriate for dealing with counterparty credit risk. In particular, as shown in Section 8.4 of [10], versions of the model are capable of generating a large range of implied volatilities for CDS spread options, broader and better behaved than with shifted CIR intensities (for results regarding the latter model we refer to [13], [14] or [16]).
- Compared to shifted CIR, the extended CIR (with piecewise constant parameter) specification allows for endogenous calibration of the term-structure of default probabilities whereas, with shifted CIR, one has to rely on arbitrary reconstruction methods. For instance, [13] uses a piecewise-linear specification of hazard rates to strip default probabilities from CDS spreads.
- The extended CIR model is very convenient when it turns to calibrate dependence parameters on CDO tranche spreads since the optimization constraints are linear (see Section 4 for more details).

Of course, extended CIR processes with piecewise constant coefficients can be seen as standard CIR processes on each time interval where the coefficients are constant. All the literature regarding simulation of standard CIR processes (in particular, how to cope with the numerical instabilities that may arise if the parameters do not satisfy a suitable Feller condition, e.g., by exact simulation based on chi-square distributions [24, Fig. 3.5 p.124]) can therefore be applied “piecewise” to such extended CIR processes.

For  $\mathbf{k} = (k_1, \dots, k_n) \in \{0, 1\}^n$ , we introduce  $\text{supp}(\mathbf{k}) = \{i \in \mathbb{N}_n; k_i = 1\}$  and  $\text{supp}^c(\mathbf{k}) = \{i \in \mathbb{N}_n; k_i = 0\}$ . Hence,  $\text{supp}(\mathbf{k})$  denotes the obligors who have defaulted in the portfolio-state  $\mathbf{k}$  and similarly  $\text{supp}^c(\mathbf{k})$  are the survived names in state  $\mathbf{k}$ . Given  $\mathbf{X} = (X^Y)_{Y \in \mathcal{Y}}$ , we aim for a model in which the predictable intensity of a jump of  $\mathbf{H} = (H^i)_{i \in \mathbb{N}_n}$  from  $\mathbf{H}_{t-} = \mathbf{k}$  to  $\mathbf{H}_t = \mathbf{l}$ , with  $\text{supp}(\mathbf{k}) \subsetneq \text{supp}(\mathbf{l})$  in  $\{0, 1\}^n$ , would be given by

$$\sum_{\{Y \in \mathcal{Y}; \mathbf{k}^Y = \mathbf{l}\}} X_t^Y, \quad (2)$$

where  $\mathbf{k}^Y$  denotes the vector obtained from  $\mathbf{k} = (k_i)_{i \in \mathbb{N}_n}$  by replacing the components  $k_i$ ,  $i \in Y$ , by numbers one. The intensity of a jump of  $\mathbf{H}$  from  $\mathbf{k}$  to  $\mathbf{l}$  at time  $t$  is thus equal to the sum of the intensities of the groups  $Y \in \mathcal{Y}$  such that, if the default of the survivors in group  $Y$  occurred at time  $t$ , the state of  $\mathbf{H}$  would move from  $\mathbf{k}$  to  $\mathbf{l}$ .

This is achieved by constructing  $\mathbf{H}$  through an  $\mathbf{X}$ -related change of probability measure, starting from a continuous-time Markov chain with intensity one (see [6]). As a result, the pair-process  $(\mathbf{X}, \mathbf{H})$  is a Markov process with respect to the filtration  $\mathcal{F}$  generated by the Brownian Motion  $\mathbf{W}$  and the random measure counting the jumps of  $\mathbf{H}$ , with infinitesimal generator  $\mathcal{A}$  of  $(\mathbf{X}, \mathbf{H})$  acting on every function  $u = u(t, \mathbf{x}, \mathbf{k})$  with  $t \in \mathbb{R}_+$ ,  $\mathbf{x} = (x_Y)_{Y \in \mathcal{Y}}$  and  $\mathbf{k} = (k_i)_{i \in \mathbb{N}_n}$  as

$$\mathcal{A}_t u(t, \mathbf{x}, \mathbf{k}) = \sum_{Y \in \mathcal{Y}} \left( a(b_Y(t) - x_Y) \partial_{x_Y} u(t, \mathbf{x}, \mathbf{k}) + \frac{1}{2} c^2 x_Y \partial_{x_Y}^2 u(t, \mathbf{x}, \mathbf{k}) + x_Y \delta_Y u(t, \mathbf{x}, \mathbf{k}) \right) \quad (3)$$

where we denote

$$\delta_Y u(t, \mathbf{x}, \mathbf{k}) = u(t, \mathbf{x}, \mathbf{k}^Y) - u(t, \mathbf{x}, \mathbf{k}).$$

---

<sup>1</sup>Note that in this regard our CIR model is a special version of the *segmented square root model* of [28], where all three coefficients of the CIR diffusion are piecewise functions of time.

## 2.1 Markov Copula Properties

Note that the SDEs for processes the  $X^Y$  have the same coefficients except for  $b_Y(t)$ , to the effect that for  $i \in \mathbb{N}_n$ ,

$$X^i := \sum_{Y \ni i} X^Y = X^{\{i\}} + \sum_{I \ni i} X^I \quad (4)$$

is again an extended CIR process, with parameters  $a$ ,  $c$  and

$$b_i(t) := \sum_{Y \ni i} b_Y(t) = b_{\{i\}}(t) + \sum_{I \ni i} b_I(t), \quad (5)$$

driven by an  $\mathcal{F}$ -Brownian motion  $W^i$  such that

$$\sqrt{X_t^i} dW_t^i = \sum_{Y \ni i} \sqrt{X_t^Y} dW_t^Y, \quad dW_t^i = \sum_{Y \ni i} \frac{\sqrt{X_t^Y}}{\sqrt{\sum_{Y \ni i} X_t^Y}} dW_t^Y. \quad (6)$$

The fact that  $W^i$  defined by (6) is an  $\mathcal{F}$ -Brownian motion results from Paul Lévy's characterization of a Brownian motion as a continuous local martingale with bracket process equal to time  $t$ . One can then check, as is done in [6], that the so-called Markov copula property holds (see [12]), in the sense that for every  $i \in \mathbb{N}_n$ ,  $(X^i, H^i)$  is an  $\mathcal{F}$ -Markov process admitting the following generator, acting on functions  $v_i = v_i(t, x_i, k_i)$  with  $(x_i, k_i) \in \mathbb{R} \times \{0, 1\}$ :

$$\begin{aligned} \mathcal{A}_t^i v_i(t, x_i, k_i) = & \quad (7) \\ & a(b_i(t) - x_i) \partial_{x_i} v_i(t, x_i, k_i) + \frac{1}{2} c^2 x_i \partial_{x_i}^2 v_i(t, x_i, k_i) + x_i (v_i(t, x_i, 1) - v_i(t, x_i, k_i)). \end{aligned}$$

Also, the  $\mathcal{F}$ -intensity process of  $H^i$  is given by  $(1 - H_t^i) X_t^i$ . In other words, the process  $M^i$  defined by,

$$M_t^i = H_t^i - \int_0^t (1 - H_s^i) X_s^i ds, \quad (8)$$

is an  $\mathcal{F}$ -martingale. Finally, the conditional survival probability function of name  $i \in \mathbb{N}_n$  is given by, for every  $t_i > t$ ,

$$\mathbb{P}(\tau_i > t_i | \mathcal{F}_t) = \mathbb{E} \left\{ \exp \left( - \int_t^{t_i} X_s^i ds \right) | X_t^i \right\}. \quad (9)$$

## 3 Pricing

Regarding the dynamics of CIR intensity processes, we assume in the sequel that the mean-reversion functions  $b_Y(t)$  are piecewise-constant with respect to a time tenor  $(T_k)_{k=1, \dots, M}$ . So, for every  $k = 1 \dots M$ ,

$$b_Y(t) = b_Y^{(k)}, \quad t \in [T_{k-1}, T_k]. \quad (10)$$

where  $b_Y^{(k)}$  is a non-negative constant and  $T_0 = 0$ . The time tenor  $(T_k)$  is a set of pillars corresponding to standard CDS maturities. In this framework, we are able to provide explicit expressions for survival probabilities of triggering events, which are the main building blocks in the calculation of CDS and CDO tranche spreads.

**Remark 3.1** For comparison purposes, the (simpler) case of deterministic time-dependent intensities will also be considered in the numerical experiments of Section 5. In that case, the default intensities will be given as  $X_t^Y := \lambda_Y(t)$  where  $\lambda_Y$  is a piecewise-constant function of time with respect to the same time tenor  $(T_k)_{k=1, \dots, M}$  as for the mean-reversion function  $b_Y$  of the CIR intensity case. Then, for every  $k = 1 \dots M$ , there exists a non-negative constant  $\lambda_Y^{(k)}$  such that

$$\lambda_Y(t) = \lambda_Y^{(k)}, \quad t \in [T_{k-1}, T_k]. \quad (11)$$

Survival probabilities (9) can be obtained explicitly in the case of piecewise-constant intensities as defined by (11). We will show now that similar analytical formulas can be obtained when the underlying intensities are driven by CIR processes with piecewise-constant mean-reversion parameters (see Proposition 3.2 and Remark 3.4).

### 3.1 Survival Probabilities of Trigger-Events

In this subsection, we provide an analytical expression for survival probabilities in an extended CIR intensity model with piecewise constant mean-reversion parameter. This allows us to compute CDS and CDO tranche spreads almost as fast as in a (deterministic) piecewise constant intensity model.

Let  $X$  be an extended CIR process with dynamics

$$dX_t = a(b(t) - X_t)dt + c\sqrt{X_t}dW_t \quad (12)$$

where  $a$  and  $c$  are positive constants and  $b(\cdot)$  is a non-negative deterministic function. Let  $\Phi$  and  $\Psi$  satisfy the following Riccati system of ODE:

$$\begin{cases} \dot{\Phi}_y(t) = -a\Phi_y(t) - \frac{c^2}{2}\Phi_y^2(t) + 1, \Phi_y(0) = y \\ \dot{\Psi}_y(t) = a\Phi_y(t), \Psi_y(0) = 0. \end{cases} \quad (13)$$

It is a classical result that these ODEs can be solved explicitly, i.e.

$$\Phi_y(t) = \frac{1 + D_y e^{-A_y t}}{B + C_y e^{-A_y t}} \quad (14)$$

$$\Psi_y(t) = \frac{a}{B} \left\{ \frac{C_y - BD_y}{A_y C_y} \log \frac{B + C_y e^{-A_y t}}{B + C_y} + t \right\}, \quad (15)$$

where  $A_y$ ,  $B$ ,  $C_y$  and  $D_y$  are given by

$$B = \frac{1}{2}(a + \sqrt{a^2 + 2c^2}), \quad C_y = (1 - By) \frac{a + c^2 y - \sqrt{a^2 + 2c^2}}{2ay + c^2 y - 2},$$

$$D_y = (B + C_y)y - 1, \quad A_y = \frac{-C_y(2B - a) + D_y(c^2 + aB)}{BD_y - C_y}.$$

**Proposition 3.2** *For any  $s \geq t$  and  $y \geq 0$ , we have:*

$$\mathbb{E}\left(e^{-\int_t^s X_u du - yX_s} | X_t = x\right) = e^{-I_{s,y}(t,x)}, \quad (16)$$

where

$$I_{s,y}(t,x) = x\Phi_y(s-t) + a \int_t^s \Phi_y(s-u)b(u)du, \quad (17)$$

and

$$\mathbb{E}\left(X_s e^{-\int_t^s X_u du} | X_t = x\right) = \partial_s I_{s,0}(t,x) e^{-I_{s,0}(t,x)}, \quad (18)$$

where the function  $\Phi$  which is implicit in  $\partial_s I$  in (18) can be computed explicitly via the first line in (13).

*Proof.* Formula (18) follows by differentiation in  $y$  and valuation at  $y = 0$  from (16). The latter formula, which is classical in the theory of (time-inhomogenous) affine processes, can also be verified by checking that  $v(t,x) := e^{-I_{s,y}(t,x)}$  satisfies the following PDE, which characterizes the left-hand side in (16) viewed as a function of  $t, x$ , for fixed  $s, y$ :

$$\partial_t v(t,x) + \mathcal{A}v(t,x) - xv(t,x) = 0, \quad v(s,x) = e^{-xy},$$

where

$$\mathcal{A}v(t, x) = a(b(t) - x)\partial_x v(t, x) + \frac{1}{2}c^2 x \partial_{x^2}^2 v(t, x)$$

is the infinitesimal generator of the affine process  $X$  in (12).  $\square$

**Remark 3.3** In case  $b(\cdot)$  is piecewise-constant, such that  $b(t) = b_k$  on every interval  $[T_{k-1}, T_k)$  of a time-grid  $(T_k)$ , then, defining  $i \leq j$  such that  $t \in [T_{i-1}, T_i)$  and  $s \in [T_{j-1}, T_j)$ , the second term in (17) is given in view of the second line in (13) by

$$\begin{aligned} a \int_t^s \Phi_y(s-u)b(u)du &= (\Psi_y(s-t) - \Psi_y(s-T_i)) b_i \\ &+ \sum_{k=i+1}^{j-1} (\Psi_y(s-T_{k-1}) - \Psi_y(s-T_k)) b_k + \Psi_y(s-T_{j-1}) b_j \end{aligned} \quad (19)$$

if  $i < j$ , otherwise  $a \int_t^s \Phi_y(s-u)b(u)du = \Psi_y(s-t)b_i$ .

**Remark 3.4** Note that the expression of survival probabilities as computed in a deterministic piecewise-constant intensity set-up can be embedded in formulas (16), (17) and (19) for suitably modified functions  $\Phi$  and  $\Psi$ . Indeed, if we assume that  $X_t := \lambda(t)$  where  $\lambda(\cdot)$  is a piecewise constant function, i.e.,  $\lambda(t) = \lambda_k$  whenever  $t \in [T_{k-1}, T_k)$ , then the relevant expression for the function  $I$  in (16) becomes

$$I_{s,y}(t, x) := (T_i - t) \lambda_i + \sum_{k=i+1}^{j-1} (T_k - T_{k-1}) \lambda_k + (s - T_{j-1} + y) \lambda_j, \quad (20)$$

which corresponds to an expression of the form (17) with  $\Phi_y(s) = 0$  and  $\Psi_y(s) = s + y$ .

## 3.2 CDS Pricing

We assume in the sequel that recovery rates are independent of default times. Under this assumption, the CDS spread of a particular name can be expressed as deterministic functions of its survival probabilities and of its expected recovery. Let  $t_1 < \dots < t_p = T$  be the remaining premium payment dates where  $T$  stands for the maturity date. We assume for simplicity that the risk-free interest rate is constant and equal to  $r$  and we denote  $\beta(t) = e^{-rt}$  the corresponding discount factor. In our numerical experiment, the current fair CDS spread of name  $i$  is approximated by the following expression

$$S_i(T) = (1 - R_i^*) \frac{\sum_{j=1}^p \beta(t_j) (\mathbb{P}(\tau_i > t_{j-1}) - \mathbb{P}(\tau_i > t_j))}{\sum_{j=1}^p \beta(t_j) (t_j - t_{j-1}) \mathbb{P}(\tau_i > t_j)} \quad (21)$$

where  $R_i^*$  denotes the expected recovery rate of name  $i$ . To derive the previous expression, we implicitly assume that, if a default occur at time  $\tau_i < T$ , the protection payment occurs at the premium payment date that immediately follows  $\tau_i$ .

Recall that (cf. (9))

$$\mathbb{P}(\tau_i > t_j) = \mathbb{E} \exp \left( - \int_0^{t_j} X_s^i ds \right) \quad (22)$$

where  $X^i$  is an extended CIR process with parameters  $a, c$  and piecewise-constant mean-reversion function  $b_i(\cdot)$  in (5) (assuming piecewise-constant functions  $b_Y(\cdot)$ ). Hence, provided the expected recovery is known, the CDS spread of name  $i$  can be efficiently calculated using part (i) of Proposition 3.2 with  $y = 0$ .

### 3.3 CDO Tranche Pricing with Random Recoveries

In this subsection we outline how to modify the model to include stochastic recoveries. Let  $\mathbf{L} = (L^i)_{1 \leq i \leq n}$  represent the  $[0, 1]^n$ -valued vector process of the loss given defaults in the pool of names. The process  $\mathbf{L}$  is a multivariate process where  $\mathbf{L}_0 \in \mathbf{0}$ , and where each component  $L_t^i$  represents the fractional loss that name  $i$  may have suffered due to default until time  $t$ . Assuming unit notional for each name, the cumulative loss process for the entire portfolio is defined as  $L_t := \sum_i (1 - R_i) H_t^i$  where the variables  $R_i$  are random and independent fractional recoveries with values in  $[0, 1]$ . The default times are defined as before, but at every time of jump of  $\mathbf{H}$ , an independent recovery draw is made for every newly defaulted name  $i$ , determining the recovery  $R_i$  of name  $i$ . In particular, the recovery rates resulting from a joint default are thus drawn independently for the affected names.

Note that independent recoveries do not break the dynamic properties developed in [6]. However by introducing stochastic recoveries we can no longer use the exact convolution recursion procedures of [7] for pricing CDO tranches. Instead we will here use an approximate procedure based on the exponential approximations of the so called hockey stick function, as presented in Iscoe et al. [26, 27] and originally developed by [4]. In this subsection we explain in detail how to use this method for computing the price of a CDO tranche in our Markov model when the individual losses are random.

The mathematical ideas underlying the method of exponential approximations were originally developed by [4], and was later adopted by Iscoe et al. in [26, 27] to price CDO tranches in a Gaussian copula model. While [26, 27] uses constant recoveries, we will in this paper adopt their techniques to random recoveries. Below we will outline the techniques given in [26, 27] and our presentation also introduces notation needed later on. First, the so called tranche loss function  $L_t^{a,b}$  for the tranche  $[a, b]$  as a function of the portfolio credit loss  $L_t$  is given by

$$L_t^{a,b} = (L_t - a)^+ - (L_t - b)^+ \quad (23)$$

where  $x^+ = \max(x, 0)$  (see Figure 1).

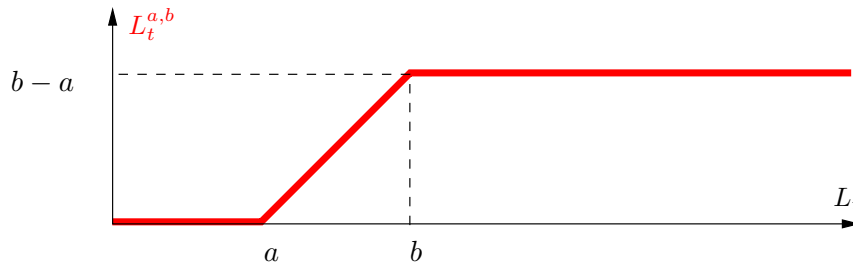


Figure 1: The tranche loss for  $[a, b]$  as function of the total loss  $L_t$ .

As in [4], we introduce the so-called hockey stick function  $h(x)$  given by

$$h(x) = \begin{cases} 1 - x & \text{if } 0 \leq x \leq 1, \\ 0 & \text{if } 1 < x \end{cases} \quad (24)$$

(see Figure 2).

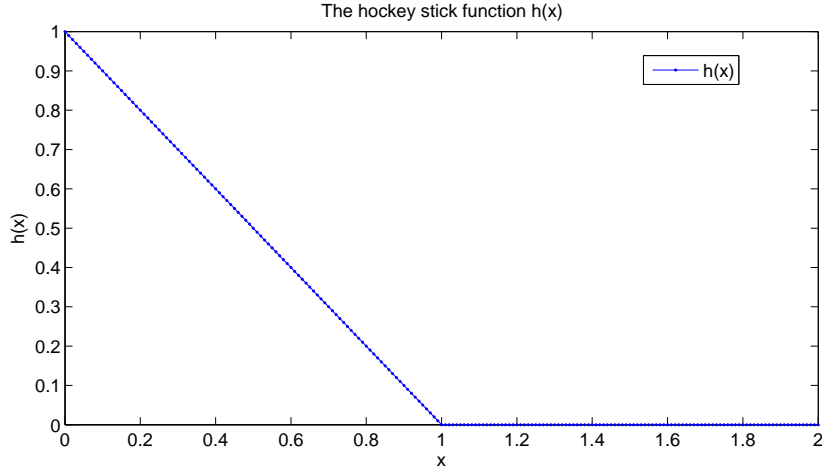


Figure 2: The hockey stick function  $h(x)$  for  $x \in [0, 2]$ .

Let  $c > 0$  be scalar. By using (24) one can show that

$$\min(x, c) = c - ch\left(\frac{x}{c}\right) \quad (25)$$

and for any two scalars  $a$  and  $b$  it holds that

$$(x - a)^+ - (x - b)^+ = \min(x, b) - \min(x, a) \quad (26)$$

so (25) and (26) then yields

$$(x - a)^+ - (x - b)^+ = b\left(1 - h\left(\frac{x}{b}\right)\right) - a\left(1 - h\left(\frac{x}{a}\right)\right). \quad (27)$$

Hence, (23) and (27) implies that

$$L_t^{a,b} = b\left(1 - h\left(\frac{L_t}{b}\right)\right) - a\left(1 - h\left(\frac{L_t}{a}\right)\right). \quad (28)$$

This observation was done by [26] which combined (28) with the results of [4]. More specifically, [4] shows that for any fixed  $\epsilon > 0$ , the function  $h(x)$  can be approximated by a function  $h_{\text{exp}}^{(q)}(x)$  on  $[0, d]$  with  $d = d(\epsilon)$  so that  $|h(x) - h_{\text{exp}}^{(q)}(x)| \leq \epsilon$  for all  $x \in [0, d]$  where  $q = q(\epsilon)$  is a positive integer and  $h_{\text{exp}}^{(q)}(x)$  is given by

$$h_{\text{exp}}^{(q)}(x) = \sum_{\ell=1}^q \omega_{\ell} \exp\left(\gamma_{\ell} \frac{x}{d}\right). \quad (29)$$

were  $(\omega_{\ell})_{\ell=1}^q$  and  $(\gamma_{\ell})_{\ell=1}^q$  are complex numbers obtained as roots of polynomials whose coefficients can be computed numerically in a straightforward way.

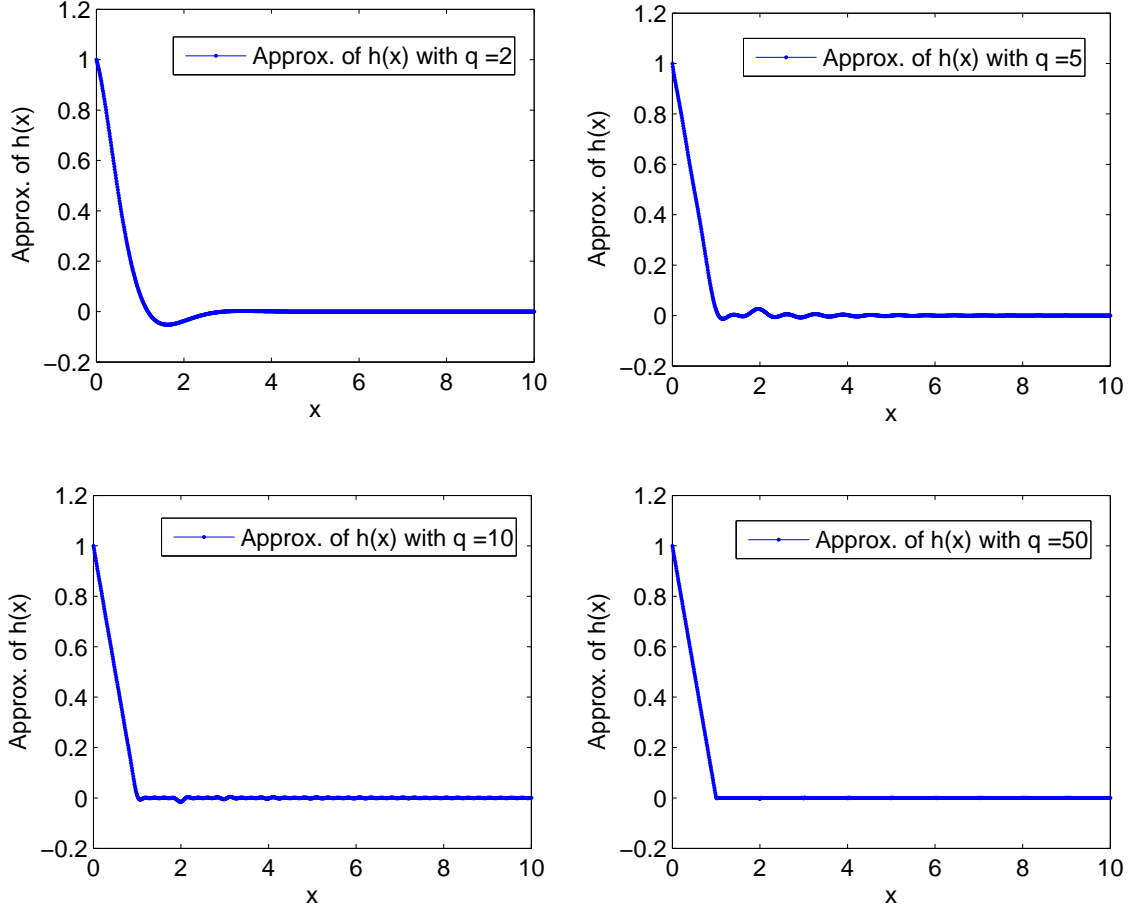


Figure 3: The function  $h_{\text{exp}}^{(q)}(x)$  as approximation of  $h(x)$  for  $x \in [0, 10]$  with  $q = 2, 5, 10$  and  $q = 50$ .

Figure 3 visualizes the approximation  $h_{\text{exp}}^{(q)}(x)$  of  $h(x)$  on  $x \in [0, 10]$  for  $q = 2, 5, 10$  and  $q = 50$ . As can be seen in Figure 3, the approximation is fairly good already for small values of  $q$ . In [26] the authors choose the algorithm for computing  $(\omega_\ell)_{\ell=1}^q$  and  $(\gamma_\ell)_{\ell=1}^q$  so that  $d(\epsilon) = 2$ , and then they show that the approximation accuracy  $\epsilon$  satisfies  $\frac{1}{4(q+1)} \leq \epsilon$  where  $q$  are the number terms in (29). Thus,  $q$  can be chosen first, implying an accuracy  $\epsilon$  so that  $\frac{1}{4(q+1)} \leq \epsilon$ . In practice, the error  $|h(x) - h_{\text{exp}}^{(q)}(x)|$  will for almost all  $x \in [0, \infty)$  be much smaller than the lower bound  $\frac{1}{4(q+1)}$  for  $\epsilon$ , as can be seen in Figure 4. More specifically, in [26, 27] the authors show that  $\text{Re}(\gamma_\ell) < 0$  for all  $\ell$  (see also in Figure 5) which implies that  $h_{\text{exp}}^{(q)}(x) \rightarrow 0$  as  $x \rightarrow \infty$  and, as pointed out by [26], since  $h(x) = 0$  for  $x \geq 1$  this guarantees that  $h_{\text{exp}}^{(q)}(x) \rightarrow h(x)$  when  $x \rightarrow \infty$ . In the rest of this paper we will, just as in [26, 27, 5], use  $d = 2$  in the approximation  $h_{\text{exp}}^{(q)}(x)$  given by (29).

Since  $(\omega_\ell)_{\ell=1}^q$  are roots to a certain polynomial, then if  $\zeta \in (\omega_\ell)_{\ell=1}^q$  it will also hold that  $\bar{\zeta} \in (\omega_\ell)_{\ell=1}^q$ . The same also holds for the complex numbers  $(\gamma_\ell)_{\ell=1}^q$ . Thus, it will hold that  $\text{Im}(\sum_{\ell=1}^q \gamma_\ell \exp(\gamma_\ell x/d)) = 0$  and Figure 5 displays the coefficients  $(\omega_\ell)_{\ell=1}^q$  and  $(\gamma_\ell)_{\ell=1}^q$  in the case  $q = 50$ .

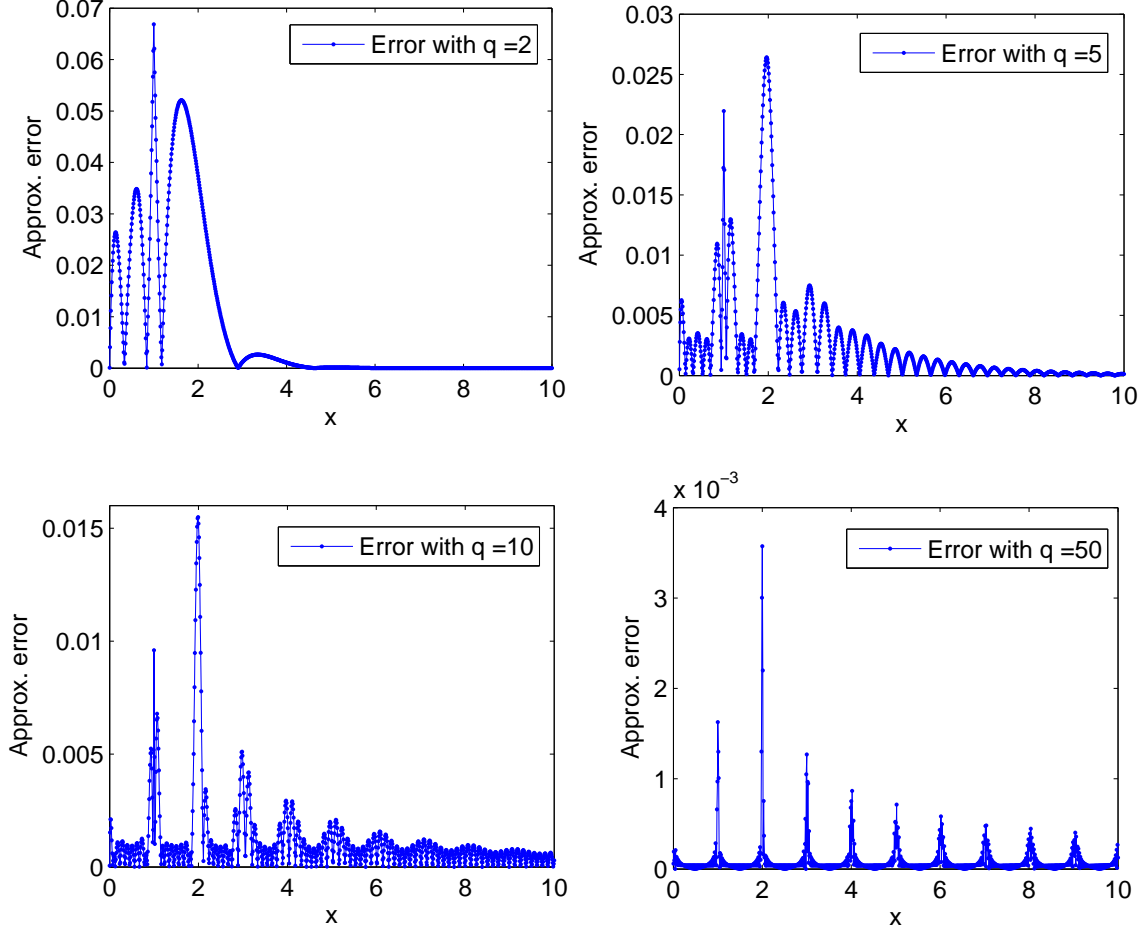


Figure 4: The approximation error  $|h(x) - h_{\text{exp}}^{(q)}(x)|$  for  $x \in [0, 10]$  with  $q = 2, 5, 10$  and  $q = 50$ .

It is well known that in order to price synthetic CDO tranches, one needs to compute the quantity  $\mathbb{E} \left[ L_t^{a,b} \right]$  for  $t > 0$ , see e.g. in [25]. So by replacing  $h(x)$  with  $h_{\text{exp}}^{(q)}(x)$  in (28) with  $d = 2$  and using (29) then implies that we can approximate  $L_t^{a,b}$  as follows

$$L_t^{a,b} \approx b - a - b \sum_{\ell=1}^q \omega_{\ell} \exp \left( \gamma_{\ell} \frac{L_t}{2b} \right) + a \sum_{\ell=1}^q \omega_{\ell} \exp \left( \gamma_{\ell} \frac{L_t}{2a} \right) \quad (30)$$

and consequently

$$\mathbb{E} \left[ L_t^{a,b} \right] \approx b - a - b \sum_{\ell=1}^q \omega_{\ell} \mathbb{E} \left[ \exp \left( \gamma_{\ell} \frac{L_t}{2b} \right) \right] + a \sum_{\ell=1}^q \omega_{\ell} \mathbb{E} \left[ \exp \left( \gamma_{\ell} \frac{L_t}{2a} \right) \right]. \quad (31)$$

Thus, in view of (31), the pricing of a CDO tranche of maturity  $T$ , boils down to computation of expectations of the form

$$\mathbb{E} e^{\gamma_{\ell} \frac{L_t}{2c}} \quad (32)$$

for  $\ell = 1, 2, \dots, q$  and different attachment points  $c$  and time horizons  $0 \leq t \leq T$ .

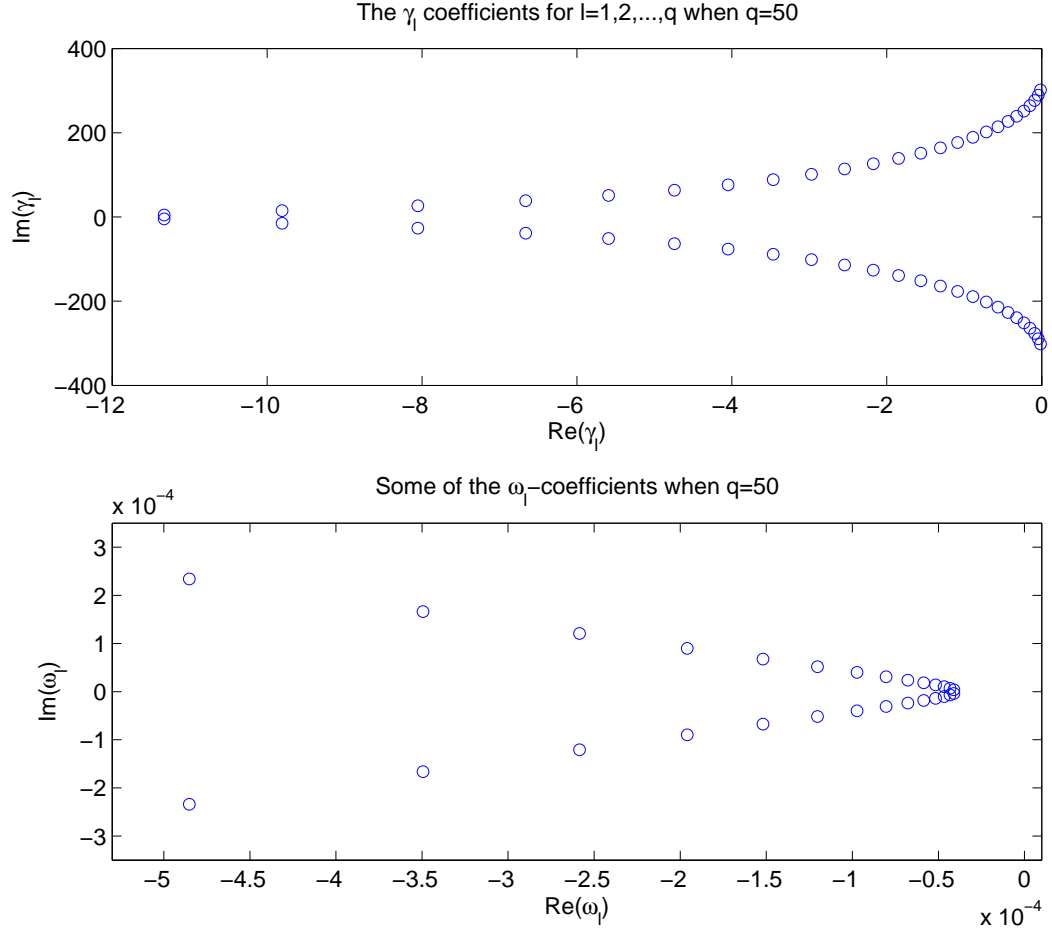


Figure 5: The coefficients  $(\gamma_\ell)_{\ell=1}^q$  (top) and some of the coefficients  $(\omega_\ell)_{\ell=1}^q$  (bottom) when  $q = 50$ .

**Remark 3.5** One can extend the present developments to conditional expectations given  $\mathcal{F}_s$  for any  $0 < s < t$ . The case  $s = 0$  is used in the calibration (our focus in this paper), while the case  $s > 0$  is needed for pricing the credit valuation adjustment (CVA) on a CDO tranche in a counterparty risky environment, a topical issue since the 2007-09 credit crisis (see [21]).

Since the algorithm for computing  $\mathbb{E}e^{\gamma_\ell \frac{L_t}{2c}}$  is the same for each  $\ell = 1, 2, \dots, q$  and any attachment point  $c$ , we will below for notational convenience simply write  $\mathbb{E}e^{\gamma L_t}$  instead of  $\mathbb{E}e^{\gamma_\ell \frac{L_t}{2c}}$ .

We now use the common shock model representation developed in Section 3 of [7], with the same notation that was introduced there except that  $\theta$  there is  $t$  here, and  $t$  there is simply 0 here, as we focus here on expectations and not conditional expectations; moreover we now use a “ $\hat{\cdot}$ ” notation for the common shocks model representation at the starting time 0 below, instead of a “ $(t)$ ” which is used for common shocks model representation with a varying forward starting time  $t$  in [5].

We thus introduce a common shocks copula model of default times  $\hat{\tau}_Y$  defined by, for every

$Y \in \mathcal{Y}$ ,

$$\widehat{\tau}_Y = \inf\{t > 0; \int_0^t X_s^Y ds > E_Y\},$$

where the random variables  $E_Y$  are i.i.d. and exponentially distributed with parameter 1. For every obligor  $i$  we let

$$\widehat{\tau}_i = \min_{\{Y \in \mathcal{Y}; i \in Y\}} \widehat{\tau}_Y, \quad (33)$$

which defines the default time of obligor  $i$  in the common shocks copula model. We also introduce the indicator processes  $\widehat{H}_t^Y = \mathbf{1}_{\{\widehat{\tau}_Y \leq t\}}$  and  $\widehat{H}_t^i = \mathbf{1}_{\{\widehat{\tau}_i \leq t\}}$ , for every triggering-event  $Y$  and obligor  $i$ . One then has much like in Proposition 2.10(ii) of [5] that

$$\mathbb{E}e^{\gamma L_t} = \mathbb{E}e^{\gamma \widehat{L}_t} \quad (34)$$

where  $\widehat{L}_t := \sum_i (1 - R_i) \widehat{H}_t^i$ .

We henceforth assume a nested structure of the sets  $I_j$  given by

$$I_1 \subset \dots \subset I_m. \quad (35)$$

This structure implies that if all obligors in group  $I_k$  have defaulted, then all obligors in group  $I_1, \dots, I_{k-1}$  have also defaulted. As detailed in [5], the nested structure (35) yields a particularly tractable expression for the portfolio loss distribution. This nested structure also makes sense financially with regards to the hierarchical structure of risks which is reflected in standard CDO tranches. Denoting conventionally  $I_0 = \emptyset$  and  $\widehat{H}_t^{I_0} = 1$ , then the event-sets

$$\widehat{\Omega}_t^j := \{\widehat{H}_t^{I_j} = 1, \widehat{H}_t^{I_{j+1}} = 0, \dots, \widehat{H}_t^{I_m} = 0\}, \quad 0 \leq j \leq m$$

form a partition of  $\Omega$  with

$$\mathbb{P}(\widehat{\Omega}_t^j) = \left(1 - \mathbb{E}e^{-\int_0^t X_s^{I_j} ds}\right) \prod_{j+1 \leq l \leq m} \mathbb{E}e^{-\int_0^t X_s^{I_l} ds}$$

where the expectations are explicitly given by Proposition 3.2(i). One then has in (34) that

$$\mathbb{E}e^{\gamma \widehat{L}_t} = \sum_{0 \leq j \leq m} \mathbb{E}(e^{\gamma \widehat{L}_t} | \widehat{\Omega}_t^j) \mathbb{P}(\widehat{\Omega}_t^j) \quad (36)$$

in which by conditional independence of the  $\widehat{H}_t^i$  given every  $\widehat{\Omega}_t^j$

$$\mathbb{E}(e^{\gamma \widehat{L}_t} | \widehat{\Omega}_t^j) = \mathbb{E}(e^{\gamma \sum_i (1-R_i) \widehat{H}_t^i} | \widehat{\Omega}_t^j) = \prod_{i \in Z} \mathbb{E}(e^{\gamma (1-R_i) \widehat{H}_t^i} | \widehat{\Omega}_t^j).$$

Now observe that by independence of  $R_i$

$$\mathbb{E}(e^{\gamma (1-R_i) \widehat{H}_t^i} | \widehat{\Omega}_t^j) = \begin{cases} \mathbb{E}e^{\gamma (1-R_i)}, & i \in I_j \\ \mathbb{E}e^{\gamma (1-R_i) \widehat{H}_t^{\{i\}}}, & \text{else} \end{cases} \quad (37)$$

with

$$\mathbb{E}e^{\gamma (1-R_i) \widehat{H}_t^{\{i\}}} = 1 - \widehat{p}_t^{i,j} \left(1 - \mathbb{E}e^{\gamma (1-R_i)}\right) \quad (38)$$

where

$$\widehat{p}_t^{i,j} = \begin{cases} 1, & i \in I_j, \\ 1 - \mathbb{E}e^{-\int_0^t X_s^{\{i\}} ds} & \text{else} \end{cases}$$

in which the expectation is explicitly given by Proposition 3.2(i) for CIR intensities or Remark 3.4 for deterministic intensities. Hence, the above formulas together with (34) will determine the quantity (32) which in turn is needed to compute the expected tranche loss given by (31). Furthermore, from the above equations we see that what is left to compute is the quantity  $\mathbb{E}e^{\gamma(1-R_i)}$  and in Subsection 5 we will give an explicitly example of the recovery rate  $R_i$  (and the quantity  $\mathbb{E}e^{\gamma(1-R_i)}$ ) which will be used in in Subsection 5.2 with the above hockey-stick method when calibrating the Markov copula against market data on CDO tranches. As will be seen in Subsection 5.2, using random recoveries will for some data sets render much better calibration results compared with the case of using constant recoveries.

## 4 Calibration with Stochastic Intensities and Constant Recovery

In this section, we discuss the calibration methodology used for fitting the stochastic intensity Markov copula model against CDO tranches on CDX.NA.IG series. We use here extended CIR intensities with piecewise-constant mean-reversion coefficients (as described previously) and we assume that recovery rates are constant. In Section 5 we will investigate the “dual” model specification where intensities are deterministic and recoveries are stochastic.

Recall that, given non-negative constants  $a$  and  $c$ , the intensity process of any group  $Y \in \mathcal{Y}$  is defined by

$$dX_t^Y = a(b_Y(t) - X_t^Y) dt + c\sqrt{X_t^Y} dW_t^Y \quad (39)$$

where  $X_0^Y$  is a given constant and  $b_Y(t)$  is a piecewise constant function such that, for every  $k = 1 \dots M$ ,  $b_Y(t) = b_Y^{(k)}$ ,  $t \in [T_{k-1}, T_k)$  with  $T_0 = 0$ . In this paper we will use a time tenor consisting of two maturities  $T_1 = 3y$  and  $T_2 = 5y$ . Moreover, in order to reduce the number of parameters at hands, we consider that, for every group  $Y \in \mathcal{Y}$ , the starting point of the corresponding intensity process is given by its first-pillar mean-reversion parameter, i.e.,  $X_0^Y = b_Y^{(1)}$ . Note that in that case, given  $a$  and  $c$ , the intensity dynamics of any group  $Y \in \mathcal{Y}$  is completely characterized by  $b_Y^{(k)}$ ,  $k = 1, 2$ . In particular, thanks to (4), the survival probability of name  $i$  up to  $T_2$  is characterized by  $(b_i^{(k)})_{k=1,2}$  where

$$b_i^{(k)} = b_{\{i\}}^{(k)} + \sum_{\mathcal{I} \ni \{i\}} b_{\mathcal{I}}^{(k)}. \quad (40)$$

The calibration is done in two steps. The first step consists in bootstrapping  $(b_i^{(k)})_{k=1,2}$  on the single-name CDS curve associated with obligor  $i$ , for any  $i = 1, \dots, n$ . The CDS curve of name  $i$  is composed of two market spreads:  $S_i^*(T_1)$  corresponding to maturity  $T_1$  and  $S_i^*(T_2)$  corresponding to maturity  $T_2$ . We first remark from (21) and Proposition 3.2 that the model spread of CDS  $i$  with maturity  $T_1$  only depends on  $b_i^{(1)}$  whereas the model spread of CDS  $i$  with maturity  $T_2$  depends on  $b_i^{(1)}$  and  $b_i^{(2)}$ . As soon as  $a$  and  $c$  are fixed, we can then find  $b_i^{(1)}$  as the solution of the non-linear (univariate) equation  $S_i(T_1) = S_i^*(T_1)$ , plugged this solution into the expression of  $S_i(T_2)$  and then find  $b_i^{(2)}$  as the solution of the non-linear (univariate) equation  $S_i(T_2) = S_i^*(T_2)$ . Figure 6 and 7 respectively show the 3y- and the 5y- implied mean-reversion coefficients bootstrapped from the 125 CDS curves of the CDX.NA.IG index constituents as of December 17, 2007. We compare three different specifications of the underlying individual intensities : piecewise-constant deterministic intensities (standard bootstrap procedure), CIR intensities with  $a = 3$  and  $c = 0.05$  and CIR intensities with  $a = 3$  and  $c = 2$ . We can see that the volatility parameter  $c$  has little impact on implied coefficients whereas individual intensities may be relatively volatile even for small volatility parameter as illustrated by Figure 8.

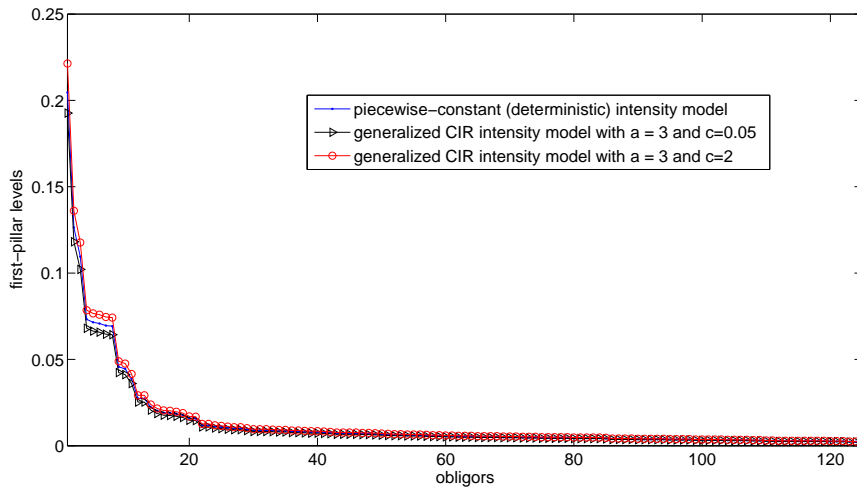


Figure 6: 3-year mean-reversion coefficients  $b_i^{(1)}$ ,  $i = 1, \dots, 125$  bootstrapped from CDX.NA.IG December 17, 2007 single-name CDS curves and sorted in decreasing order.

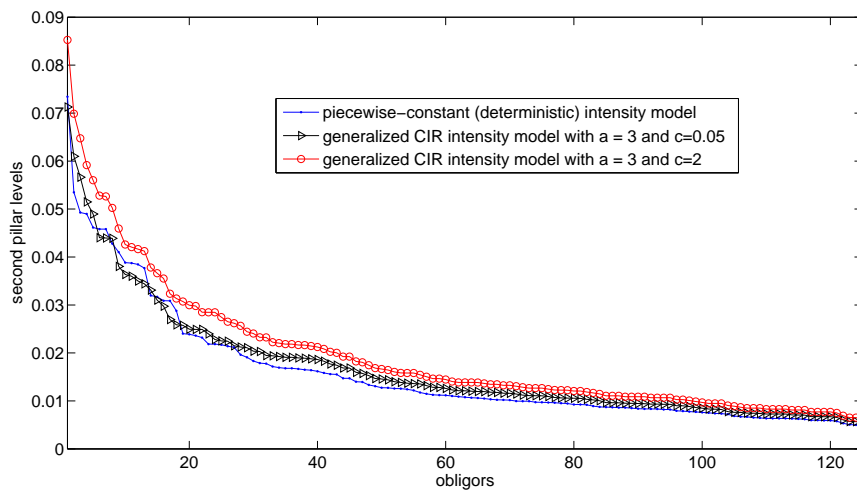


Figure 7: 5-year mean-reversion coefficients  $b_i^{(2)}$ ,  $i = 1, \dots, 125$  bootstrapped from CDX.NA.IG December 17, 2007 single-name CDS curves and sorted in decreasing order.

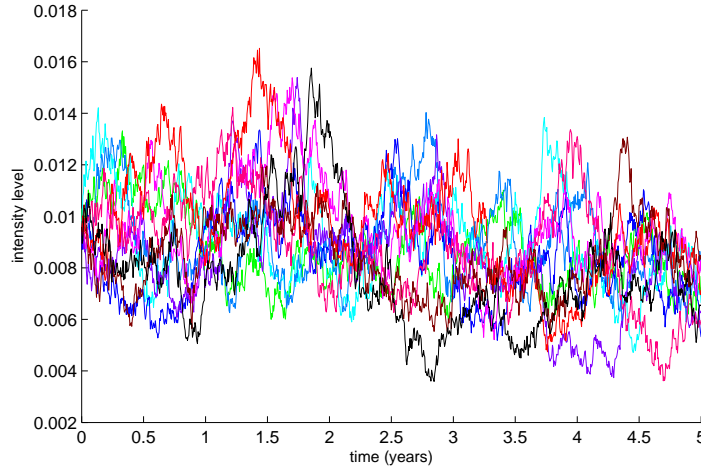


Figure 8: Sample paths of generalized CIR intensities with  $a = 3$  and  $c = 0.05$  where mean-reversion parameters are implied from AIG CDS curve at December 17, 2007. The first and the second pillar coefficients are (resp.) equal to  $b^{(1)} = 0.096$  and  $b^{(2)} = 0.075$ .

**Remark 4.1** We checked that, for  $a = 3$  and  $c = 0.05$ , the Feller's condition holds for all names after calibration of the mean-reversion levels  $b^{(k)}$ 's on CDS spreads. This eases Monte Carlo path generation considerably compared to a situation where the Feller's condition would be violated.

The second step is to calibrate group parameters  $(b_{I_j}^{(k)})_{k=1,2}, j = 1, \dots, m$  so that the model CDO tranche spreads coincide with the corresponding market spreads. The hockey-stick method described in Subsection 3.3 can be used to compute model CDO tranche spreads.

Moreover, in view of (40), we impose that, for all  $k = 1, 2$  and  $i = 1, \dots, n$ , the group parameters are such that

$$\sum_{\mathcal{I} \ni I \ni i} b_I^{(k)} \leq b_i^{(k)} \quad (41)$$

for all  $i = 1, \dots, 125$ . The previous constraints guarantee that the long-term averages  $b_{\{i\}}^{(k)}$  of single-group intensities are all positive. This in turn implies by construction that the starting points of single-group intensities  $X_0^{\{i\}}$  are all positive. Given the nested structure of the groups  $I_j$ -s specified in (35), the following constrains must hold for all  $l = 1, \dots, m$  and  $k = 1, 2$ :

$$\sum_{j=l}^m b_{I_j}^{(k)} \leq \min_{i \in I_l \setminus I_{l-1}} b_i^{(k)}. \quad (42)$$

Next, the group parameters  $\mathbf{b} = (b_{I_j}^{(k)})_{j,k} = \{b_{I_j}^{(k)} : j = 1, \dots, m \text{ and } k = 1, 2\}$  are then calibrated so that the five-year model spread  $S_{a_l, b_l}(\boldsymbol{\lambda}) =: S_l(\boldsymbol{\lambda})$  will coincide with the corresponding market spread  $S_l^*$  for each tranche  $l$ . To be more specific, the parameters  $\mathbf{b} = (b_{I_j}^{(k)})_{j,k}$  are obtained according to

$$\mathbf{b} = \underset{\hat{\mathbf{b}}}{\operatorname{argmin}} \sum_l \left( \frac{S_l(\hat{\mathbf{b}}) - S_l^*}{S_l^*} \right)^2 \quad (43)$$

under the constraints that all elements in  $\mathbf{b}$  are nonnegative and that  $\mathbf{b}$  satisfies the inequalities (42). In  $S_l(\hat{\mathbf{b}})$  we have emphasized that the model spread for tranche  $l$  is a function of  $\mathbf{b} = (b_{I_j}^{(k)})_{j,k}$  but we suppressed the dependence in other parameters like interest rate, payment frequency or  $b_i$ ,  $i = 1, \dots, n$ . In the calibration we used an interest rate of 3%, the payments in the premium leg

were quarterly and the integral in the default leg was discretized on a quarterly mesh. We use a constant recovery of 40%.

Table 1: CDX.NA.IG Series 9, December 17, 2007. The market and model spreads and the corresponding absolute errors, both in bp and in percent of the market spread. The  $[0, 3]$  spread is quoted in %. All maturities are for five years.

Tranche	$[0, 3]$	$[3, 7]$	$[7, 10]$	$[10, 15]$	$[15, 30]$
Market spread	48.07	254.0	124.0	61.00	41.00
Model spread	50.37	258.01	124.68	61.32	41.91
Absolute error in bp	2.301	4.016	0.684	0.327	0.912
Relative error in %	4.787	1.581	0.552	0.536	2.225

As can be seen in Table 1, we obtain a correct fit for CDX 2007-12-17 even in the case where no name is removed from the calibration constraints. Here, we use 5 groups  $I_1, I_2, \dots, I_5$  where  $I_j = \{1, \dots, i_j\}$  for  $i_j = 8, 19, 27, 102, 125$ . However, for the two cases, we label the obligors by decreasing level of riskiness. We use the average over 3-year and 5-year CDS spreads as a measure of riskiness. Consequently, obligor 1 has the highest average CDS spread while company 125 has the lowest average CDS spread. We use Matlab in our numerical calculations and the related objective function is minimized under the suitable constraints by using the built in optimization routine `fmincon` (e.g. in this setup, minimizing the criterion (43) under the constraints given by equations on the form (42)).

For iTraxx Europe 2008-03-31, the calibration results are not improved with respect to the piecewise-constant intensity model and constant recovery.

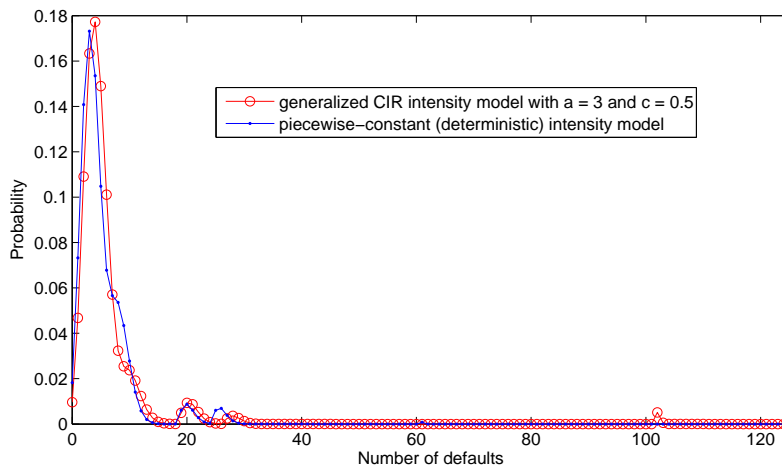


Figure 9: Comparison of 5-year implied loss distributions ( $\mathbb{P}(\sum_i H_t^i = k)$ ,  $k = 0, \dots, 125$ ) from CDX.NA.IG December 17, 2007 calibration of the generalized CIR intensity model and the piecewise constant intensity model.

As a matter of comparison, we plot in Figure 9 the loss distribution functions obtained from fitted parameters of the generalized CIR intensity model with  $a = 3$  and  $c = 0.5$  and from the fitted

parameters of the piecewise-constant (deterministic) intensity model (see Subsection 5.2 for more details). Note that the grouping is not the same in the two calibrated models. For the deterministic intensity model, we used 5 groups  $I_1, I_2, \dots, I_5$  where  $I_j = \{1, \dots, i_j\}$  for  $i_j = 6, 19, 25, 61, 125$  when calibrating the joint default intensities. Moreover, the obligors in the set  $I_5 \setminus I_4$  consisting of the 64 safest companies are assumed to never default individually, and the corresponding CDSs are excluded from the calibrations constraints. This specification renders a perfect fit. For the CIR intensity model, we also use 5 groups but with  $i_j = 8, 19, 27, 102, 125$  and, contrary to the deterministic intensity model, we do not remove any name from the calibration constraints. This specification renders a very good fit.

## 5 Calibration with Deterministic Intensities and Random Recoveries

In this section we discuss the second calibration methodology used when fitting the Markov copula model against CDO tranches on the iTraxx Europe and CDX.NA.IG series in Subsection 5.2. This method relies on piecewise constant default intensities and random recoveries. Recall that compared with constant recoveries, using random recoveries requires a more sophisticated method in order to compute the expected tranche losses, as was explained in Subsection 3.3.

The piecewise-constant intensity model used in this section is the one presented in Remark 3.1 (see also numerical applications in [7]). Remark 3.4 can be used to compute survival probabilities in this setting.

The calibration methodology and constraints connected to the piecewise constant default intensities are the same as for the mean-reversion coefficients in the CIR intensity case of Section 4: one only needs to replace  $b$  by  $\lambda$  in formulas (40), (41) and (42). Therefore we will in this Section only discuss the distribution for the individual stochastic recoveries  $R_i$  as well as accompanying constraints used in the calibration. This distribution will determine the quantity  $\mathbb{E}(e^{\gamma(1-R_i)})$  in (38) which is needed to compute the expected tranche losses.

### 5.1 Random recoveries specification and calibration methodology

We assume that the individual recoveries  $\{R_i\}$  are i.i.d and have a binomial mixture distribution of the following form

$$R_i \sim \frac{1}{K} \text{Bin}(K, R^*(p_0 + (1 - \Theta)p_1)) \quad \text{where } \Theta \in \{0, 1\} \quad \text{and } \mathbb{P}[\Theta = 1] = q \quad (44)$$

where  $R^*$ ,  $q$ ,  $p_0$  and  $p_1$  are positive constants and  $K$  is an integer (in this paper and in [5] we let  $K = 10$ ). As a result, the distribution function for the recovery rate is given by

$$\mathbb{P}\left[R_i = \frac{k}{K}\right] = \sum_{\xi=0}^1 \mu(\xi) \binom{K}{k} p(\xi)^k (1 - p(\xi))^{K-k} \quad \text{where } p(\xi) = R^*(p_0 + (1 - \xi)p_1) \quad (45)$$

where  $\xi \in \{0, 1\}$  and  $\mu(1) = q$ ,  $\mu(0) = 1 - q$ .

In view of (44) and (45) we can give an explicit expression for the quantity  $\mathbb{E}e^{\gamma(1-R_i)}$  specified in Subsection 3.3, as follows

$$\mathbb{E}e^{\gamma(1-R_i)} = \sum_{\xi=0}^1 \sum_{k=0}^K e^{\gamma(1-\frac{k}{K})} \binom{K}{k} p(\xi)^k (1 - p(\xi))^{K-k}. \quad (46)$$

Recall that  $\mathbb{E}e^{\gamma(1-R_i)}$  together with the corresponding computations in Subsection 3.3 and Equation (34) will determine the quantity  $\mathbb{E}e^{\gamma\epsilon\frac{L_t}{2c}}$  in (32) which in turn is needed to compute the expected tranche loss given by Equation (31).

Let  $R^*$  be a constant representing the average recovery for each obligor in the portfolio. We now impose the constraint  $\mathbb{E}[R] = R^*$  which is necessary in order to have a calibration of the

single-name CDSs that is separate from the calibration of the common-shock parameters. The condition  $\mathbb{E}[R] = R^*$  leads to constraints on the parameters  $p_0$ ,  $q$  and  $p_1$  that must be added to the constraints for the common shock intensities used in the calibration of the CDO tranches (recall that the calibration is a constrained minimization problem for these parameters). Below we derive these constraints for  $p_0$ ,  $q$  and  $p_1$ . First, note that

$$\mathbb{E}[R] = \frac{R^*}{K} K \mathbb{E}[p_0 + (1 - \xi)p_1] = R^*p_0 + (1 - q)p_1$$

so the condition  $\mathbb{E}[R] = R^*$  implies  $p_0 + (1 - q)p_1 = 1$  which yields

$$p_1 = \frac{1 - p_0}{1 - q}. \quad (47)$$

Thus,  $p_1$  can be seen as a function of  $q$  and  $p_0$ . Next, in view of (44) we have for any scalar  $\xi \in \{0, 1\}$  that

$$\mathbb{P}\left[R = \frac{k}{K} \mid \Theta = \xi\right] = \binom{K}{k} p(\xi)^k (1 - p(\xi))^{K-k} \quad (48)$$

where  $p(\xi)$  is defined as in (45). Since  $p(\xi)$  is a probability for  $\xi \in \{0, 1\}$  it must hold that

$$p(1) = R^*p_0 \in (0, 1) \quad \text{and} \quad p(0) = R^*(p_0 + p_1) \in (0, 1)$$

that is,

$$0 < R^*p_0 < 1 \quad \text{and} \quad 0 < R^*(p_0 + p_1) < 1. \quad (49)$$

We can always assume that  $p_0 > 0$  and  $0 < R^* < 1$  so the first condition in (49) then implies

$$p_0 < \frac{1}{R^*}. \quad (50)$$

Furthermore, by inserting (47) into the second condition in (49) we retrieve the following constraint

$$0 < R^* \frac{1 - p_0 q}{1 - q} < 1. \quad (51)$$

Since  $q \in (0, 1)$  and consequently  $1 - q > 0$ , then (51) implies  $1 - p_0 q > 0$ , that is

$$q < \frac{1}{p_0}. \quad (52)$$

However, we note that this is a “soft” condition since (50) implies that  $p_0 < \frac{1}{R^*}$  and if  $p_0 < 1$  then (52) is superfluous since we already know that  $0 < q < 1$ . Next, (51) also tells us that  $R^*(1 - p_0 q) < (1 - q)$  which after some computation yields

$$q < \frac{1 - R^*}{1 - R^*p_0}. \quad (53)$$

Finally, it must obviously hold that  $q < 1$  since  $\mathbb{P}[\Theta = 1] = q$ . Thus, combining this with (52) and (53) gives us the following final constraint for the parameter  $q$ ,

$$q < \min\left(1, \frac{1}{p_0}, \frac{1 - R^*}{1 - R^*p_0}\right). \quad (54)$$

Consequently, using the same notation as in Section 4 and replacing the group parameters identifier  $\mathbf{b}$  by  $\boldsymbol{\lambda} = (\lambda_{I_j}^{(k)})_{j,k} = \{\lambda_{I_j}^{(k)} : j = 1, \dots, m \text{ and } k = 1, 2\}$ , the parameters  $\boldsymbol{\theta} = (\boldsymbol{\lambda}, q)$  are obtained according to

$$\boldsymbol{\theta} = \underset{\hat{\boldsymbol{\theta}}}{\operatorname{argmin}} \sum_l \left( \frac{S_l(\hat{\boldsymbol{\theta}}) - S_l^*}{S_l^*} \right)^2 \quad (55)$$

where  $\lambda$  must satisfy the same constraints as  $\mathbf{b}$  in Section 4 and  $q$  must obey (54). The rest of the notation in (55) are defined as in Section 4. In our calibrations the parameters  $p_0$  and  $R^*$  will be treated as exogenously given parameters where we set  $R^* = 40\%$  while  $p_0$  can be any positive scalar satisfying  $p_0 < \frac{1}{R^*}$ . The scalar  $p_0$  will give us some freedom to fine-tune our calibrations. In Subsection 5.2 we use the above setting with stochastic recoveries when calibrating this model against two different CDO data-sets.

Finally, note that if the i.i.d recoveries  $R_i$  would follow other distributions than (44) we simply modify  $\mathbb{E}e^{\gamma(1-R_i)}$  in (38) in Subsection 3.3 but the rest of the computations are the same. Of course, changing (44) will also imply that the constraints in (54) will no longer be relevant.

## 5.2 Calibration Results

In all the numerical calibrations below we use an interest rate of 3%, the payments in the premium leg are quarterly and the integral in the default leg is discretized on a quarterly mesh. Constant or average recoveries (as relevant) are set equal to 40%.

In this subsection we calibrate our model against CDO tranches on the iTraxx Europe and CDX.NA.IG series with maturity of five years. We use the random recoveries and the calibration methodology as described in Subsection 5.1. Hence, the 125 single-name CDSs constituting the entities in these series are bootstrapped from their market spreads for  $T_1 = 3$  and  $T_2 = 5$  using piecewise constant individual default intensities on the time intervals  $[0, 3]$  and  $[3, 5]$ . Figure 10 displays the 3 and 5-year market CDS spreads for the 125 obligors used in the single-name bootstrapping, for the two portfolios CDX.NA.IG sampled on December 17, 2007 and the iTraxx Europe series sampled on March 31, 2008. The CDS spreads are sorted in decreasing order.

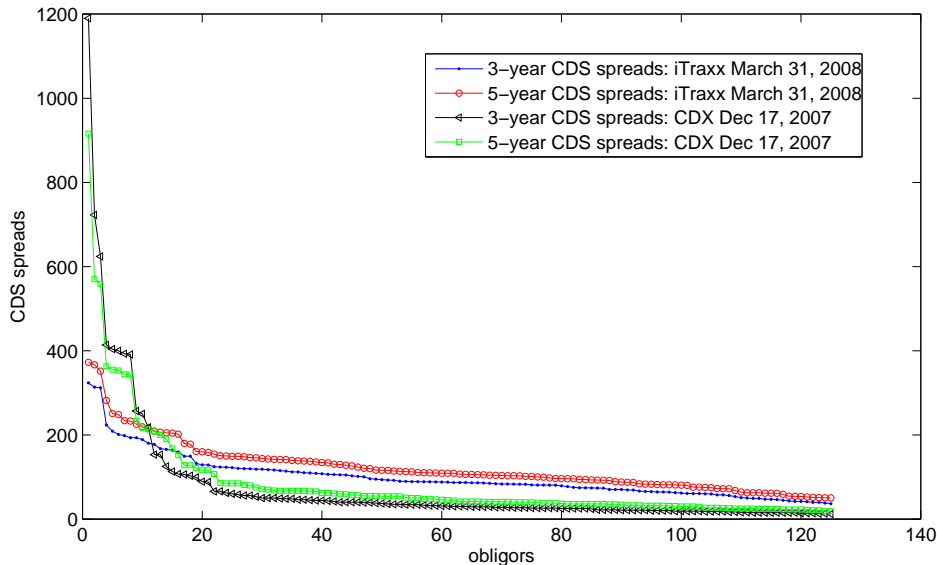


Figure 10: The 3 and 5-year market CDS spreads for the 125 obligors used in the single-name bootstrapping, for the two portfolios CDX.NA.IG sampled on December 17, 2007 and the iTraxx Europe series sampled on March 31, 2008. The CDS spreads are sorted in decreasing order.

When calibrating the joint default intensities  $\lambda = (\lambda_{I_j}^{(k)})_{j,k}$  for the CDX.NA.IG Series 9, December 17, 2007 we used 5 groups  $I_1, I_2, \dots, I_5$  where  $I_j = \{1, \dots, i_j\}$  for  $i_j = 6, 19, 25, 61, 125$ . Recall that we label the obligors by decreasing level of riskiness. We use the average over 3-year

and 5-year CDS spreads as a measure of riskiness. Consequently, obligor 1 has the highest average CDS spread while company 125 has the lowest average CDS spread. Moreover, the obligors in the set  $I_5 \setminus I_4$  consisting of the 64 safest companies are assumed to never default individually, and the corresponding CDSs are excluded from the calibration, which in turn relaxes the constraints for  $\lambda$ . Hence, the obligors in  $I_5 \setminus I_4$  can only bankrupt due to a simultaneous default of the companies in the group  $I_5 = \{1, \dots, 125\}$ , i.e., in an Armageddon event. With this structure the calibration against the December 17, 2007 data-set is very good as can be seen in Table 2. By using stochastic recoveries specified as in (44) and (45) we get a perfect fit of the same data-set. The calibrated common shock intensities  $\lambda$  for the 5 groups in the December 17, 2007 data-set, both for constant and stochastic recoveries, are displayed in the left subplot in Figure 11. Note that the shock intensities  $\lambda_{I_j}^{(1)}$  for the first pillar (i.e. on the interval  $[0, 3]$ ) follows the same trends both in the constant and stochastic recovery case, while the shock intensities  $\lambda_{I_j}^{(2)}$  for the second pillar (i.e. on the interval  $[3, 5]$ ) has less common trend.

Table 2: CDX.NA.IG Series 9, December 17, 2007 and iTraxx Europe Series 9, March 31, 2008. The market and model spreads and the corresponding absolute errors, both in bp and in percent of the market spread. The  $[0, 3]$  spread is quoted in %. All maturities are for five years.

CDX 2007-12-17: Calibration with constant recovery					
Tranche	[0, 3]	[3, 7]	[7, 10]	[10, 15]	[15, 30]
Market spread	48.07	254.0	124.0	61.00	41.00
Model spread	48.07	254.0	124.0	61.00	38.94
Absolute error in bp	0.010	0.000	0.000	0.000	2.061
Relative error in %	0.0001	0.000	0.000	0.000	5.027

CDX 2007-12-17: Calibration with stochastic recovery					
Tranche	[0, 3]	[3, 7]	[7, 10]	[10, 15]	[15, 30]
Market spread	48.07	254.0	124.0	61.00	41.00
Model spread	48.07	254.0	124.0	61.00	41.00
Absolute error in bp	0.000	0.000	0.000	0.000	0.000
Relative error in %	0.000	0.000	0.000	0.000	0.000

iTraxx Europe 2008-03-31: Calibration with constant recovery					
Tranche	[0, 3]	[3, 6]	[6, 9]	[9, 12]	[12, 22]
Market spread	40.15	479.5	309.5	215.1	109.4
Model spread	41.68	429.7	309.4	215.1	103.7
Absolute error in bp	153.1	49.81	0.0441	0.0331	5.711
Relative error in %	3.812	10.39	0.0142	0.0154	5.218

iTraxx Europe 2008-03-31: Calibration with stochastic recovery					
Tranche	[0, 3]	[3, 6]	[6, 9]	[9, 12]	[12, 22]
Market spread	40.15	479.5	309.5	215.1	109.4
Model spread	40.54	463.6	307.8	215.7	108.3
Absolute error in bp	39.69	15.90	1.676	0.5905	1.153
Relative error in %	0.9886	3.316	0.5414	0.2745	1.053

The calibration of the joint default intensities  $\lambda = (\lambda_{I_j}^{(k)})_{j,k}$  for the data sampled at March

31, 2008 is more demanding. This time we use 18 groups  $I_1, I_2, \dots, I_{18}$  where  $I_j = \{1, \dots, i_j\}$  for  $i_j = 1, 2, \dots, 11, 13, 14, 15, 19, 25, 79, 125$ . In order to improve the fit, as in the 2007-case, we relax the constraints for  $\lambda$  by excluding from the calibration the CDSs corresponding to the obligors in  $I_{18} \setminus I_{17}$ . Hence, we assume that the obligors in  $I_{18} \setminus I_{17}$  never default individually, but can only bankrupt due to an simultaneous default of all companies in the group  $I_{18} = \{1, \dots, 125\}$ . In this setting, the calibration of the 2008 data-set with constant recoveries yields an acceptable fit except for the [3,6] tranche, as can be seen in Table 2. However, by including stochastic recoveries (44), (45) the fit is substantially improved as seen in Table 2. Furthermore, in both recovery versions, the more groups added the better the fit, which explain why we use as many as 18 groups.

The calibrated common shock intensities  $\lambda$  for the 18 groups in the March 2008 data-set, both for constant and stochastic recoveries, are displayed in the right subplot in Figure 11. In this subplot we note that for the 13 first groups  $I_1, \dots, I_{13}$ , the common shock intensities  $\lambda_{I_j}^{(1)}$  for the first pillar are identical in the constant and stochastic recovery case, and then diverge quite a lot on the last five groups  $I_{14}, \dots, I_{18}$ , except for group  $I_{16}$ . Similarly, in the same subplot we also see that for the 11 first groups  $I_1, \dots, I_{11}$ , the shock intensities  $\lambda_{I_j}^{(2)}$  for the second pillar are identical in the constant and stochastic recovery case, and then differ quite a lot on the last seven groups, except for group  $I_{13}$ .

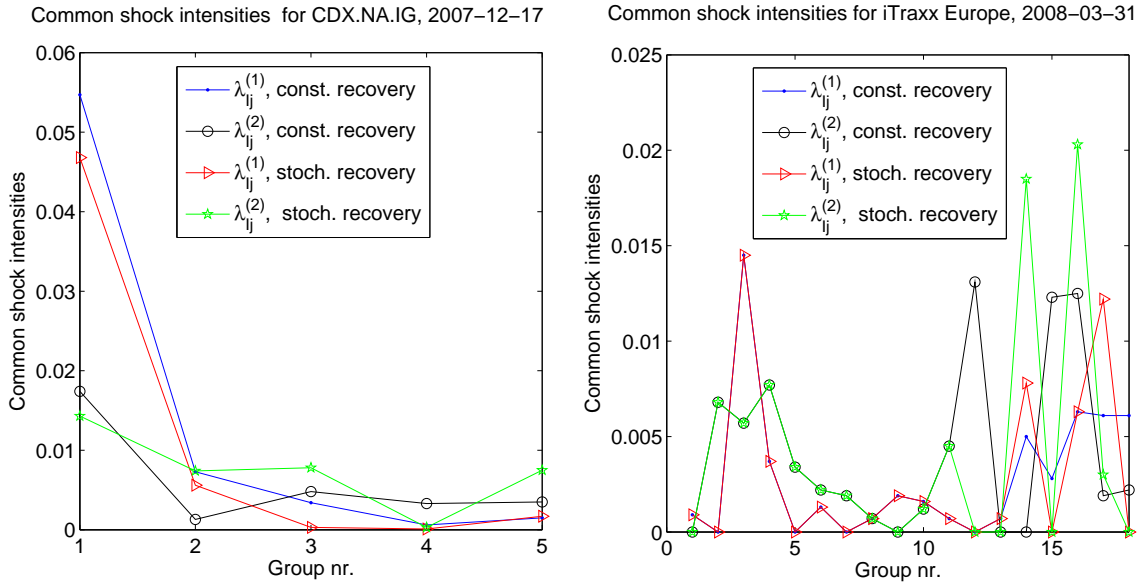


Figure 11: The calibrated common shock intensities  $(\lambda_{I_j}^{(k)})_{j,k}$  both in the constant and stochastic recovery case for the two portfolios CDX.NA.IG sampled on December 17, 2007 (left) and the iTraxx Europe series sampled on March 31, 2008 (right).

The optimal parameters  $q$  and  $p_0$  used in the stochastic recovery model was given by  $q = 0.4405$  and  $p_0 = 0.4$  for the 2007 data set and  $q = 0.6002$  and  $p_0 = 0.4$  for the 2008 case. Figure 12 displays the recovery distribution with calibrated parameters  $q$  for the two different data sets CDX.NA.IG series sampled at 2007-12-07 and iTraxx Europe sampled at 2008-03-31. Here  $\mathbb{E}[R] = R^* = 0.4$  and  $p_0 = 0.4$  in both cases. As seen in Figure 12, the implied probability for a recovery of 0%, 10% and 20% was consistently higher in the 2008 sample compared with the 2007 data set (in March 2008 Bear Stearns was bailed out leading to around three times higher credit spreads than in December 2007, both in Europe and North America). Recall that a recovery of 0% means that everything is lost at a default.

Let us finally discuss the choice of the groupings  $I_1 \subset I_2 \subset \dots \subset I_m$  in our calibrations. First, for the CDX.NA.IG Series 9, December 17, 2007 data set, we used  $m = 5$  groups with as

always  $i_m = n$ . For  $j = 1, 2$  and  $4$  the choice of  $i_j$  corresponds to the number of defaults needed for the loss process with constant recovery of 40% to reach the  $j$ -th attachment points. Hence,  $i_j \cdot \frac{1-R}{n}$  with  $R = 40\%$  and  $n = 125$  then approximates the attachment points 3%, 10%, 30% which explains the choice  $i_1 = 6, i_2 = 19, i_4 = 61$ . The choice of  $i_3 = 25$  implies a loss of 12% and gave a better fit than choosing  $i_3$  to exactly match 15%. Finally, no group was chosen to match the attachment point of 7% since this made the calibration worse off for all groupings we tried. With the above grouping structure we got almost perfect fits in the constant recovery case, and perfect fit with stochastic recovery, as was seen in Table 2. Unfortunately, using the same technique on the market CDO data from the iTraxx Europe series sampled on March 31, 2008 was not enough to achieve good calibrations. Instead more groups had to be added and we tried different groupings which led to the optimal choice rendering the calibration in Table 2. To this end, it is of interest to study the sensitivity of the calibrations with respect to the choice of the groupings on the form  $I_1 \subset I_2 \subset \dots \subset I_m$  where  $I_j = \{1, \dots, i_j\}$  for  $i_j \in \{1, 2, \dots, m\}$  and  $i_1 < \dots < i_m = 125$  on the March 31, 2008, data set. Three such groupings are displayed in Table 3 and the corresponding calibration results on the 2008 data set is showed in Table 4. From Table 4 we see that in the case with constant recovery the relative calibration error in percent of the market spread decreased monotonically for the first three tranches as the number of groups increased. Furthermore, in the case with stochastic recovery the relative calibration error decreased monotonically for all five tranches as the number of groups increased in each grouping. The rest of the parameters in the calibration were the same as in the calibration in Table 2.

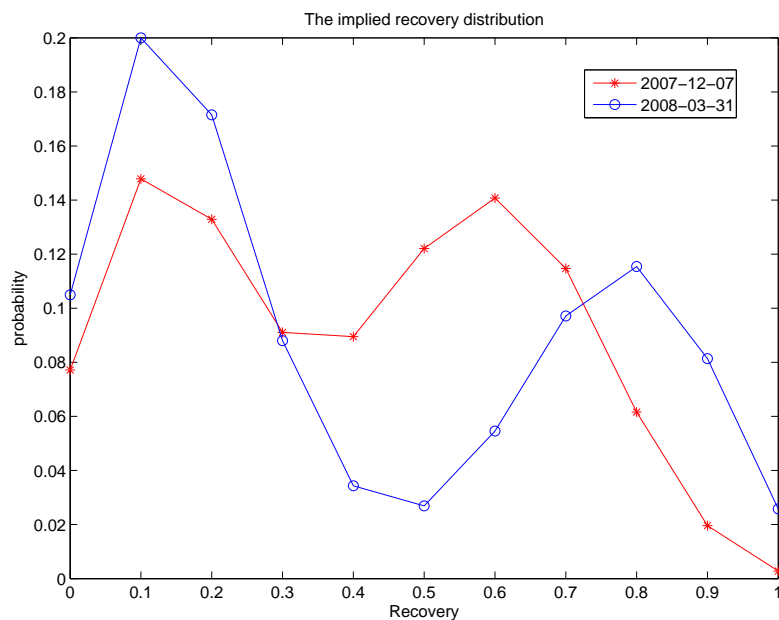


Figure 12: The implied recovery distribution with calibrated parameters  $q$  in [5], for the two different data sets CDX.NA.IG series sampled at 2007-12-07 and iTraxx Europe sampled at 2008-03-31, where  $\mathbb{E}[R] = R^* = 0.4$  in both cases.

Table 3: Three different groupings (denoted A,B and C) consisting of  $m = 7, 9, 13$  groups having the structure  $I_1 \subset I_2 \subset \dots \subset I_m$  where  $I_j = \{1, \dots, i_j\}$  for  $i_j \in \{1, 2, \dots, m\}$  and  $i_1 < \dots < i_m = 125$ .

Three different groupings													
$i_j$	$i_1$	$i_2$	$i_3$	$i_4$	$i_5$	$i_6$	$i_7$	$i_8$	$i_9$	$i_{10}$	$i_{11}$	$i_{12}$	$i_{13}$
Grouping A	6	14	15	19	25	79	125						
Grouping B	2	4	6	14	15	19	25	79	125				
Grouping C	2	4	6	8	9	10	11	14	15	19	25	79	125

Finally, we remark that the two optimal groupings used in Table 2 in the two different data sets CDX.NA.IG Series 9, December 17, 2007 and iTraxx Europe Series 9, March 31, 2008 differ quite a lot. However, the CDX.NA.IG Series is composed by North American obligors while the iTraxx Europe Series is formed by European companies. Thus, there is no model risk or inconsistency created by using different groupings for these two different data sets, coming from two disjoint markets. If on the other hand the same series is calibrated and assessed (e.g. for hedging) at different time points in a short time span, it is of course desirable to use the same grouping in order to avoid model risk.

Table 4: The relative calibration error in percent of the market spread, for the three different groupings A, B and C in Table 3, when calibrated against CDO tranche on iTraxx Europe Series 9, March 31, 2008 (see also in Table 2).

Relative calibration error in % (constant recovery)					
Tranche	[0, 3]	[3, 6]	[6, 9]	[9, 12]	[12, 22]
Error for grouping A	6.875	18.33	0.0606	0.0235	4.8411
Error for grouping B	6.622	16.05	0.0499	0.0206	5.5676
Error for grouping C	4.107	11.76	0.0458	0.0319	3.3076

Relative calibration error in % (stochastic recovery)					
Tranche	[0, 3]	[3, 6]	[6, 9]	[9, 12]	[12, 22]
Error for grouping A	3.929	9.174	2.902	1.053	2.109
Error for grouping B	2.962	7.381	2.807	1.002	1.982
Error for grouping C	1.439	4.402	0.5094	0.2907	1.235

## Conclusions and Perspectives

In this paper we make a focus on two practically important features of the Markov copula portfolio credit risk model of [5, 6, 7]: random recoveries and stochastic intensities. Regarding random recoveries it would be interesting to find ways to add some dependence features without breaking the model tractability (in the current specifications one is only able to work with independent recoveries). As for stochastic intensities it would nice to find a good way of fixing the parameters  $a$  and  $c$ , maybe based on historical observation of the dynamics of CDS spreads, rather than quite arbitrarily in this paper, as these dynamic parameters have little impact on CDS and CDO spreads. Also note that other specification of the intensities could be used, in particular Lévy Hull-White intensities driven by subordinators (for the sake of non-negativity, cf. Example 3.6 in [20]). Finally it would be interesting to apply these alternative specifications and to compare them in the context of CVA computations on portfolios of CDS and/or CDOs.

## References

- [1] ANDERSEN, L. AND SIDENIUS, J.: Extensions to the Gaussian Copula: Random Recovery and Random Factor Loadings, *Journal of Credit Risk*, Vol. 1, No. 1 (Winter 2004), p. 29–70.
- [2] BIELECKI, T., BRIGO, D., CRÉPEY, S.: *Counterparty Risk Modeling – Collateralization, Funding and Hedging*, Taylor & Francis (in preparation).
- [3] ASSEFA, S., BIELECKI, T.R., CRÉPEY, S. AND JEANBLANC, M.: CVA computation for counterparty risk assessment in credit portfolios. *Credit Risk Frontiers*, Bielecki, T.R., Brigo, D. and Patras, F., eds., Wiley/Bloomberg-Press, 2011.
- [4] BEYLKIN, G. AND MONZON, L. On approximation of functions by exponential sums, *Applied and Computational Harmonic Analysis*, **19**(1): 17-48, 2005.
- [5] BIELECKI, T.R., COUSIN, A., CRÉPEY, S., HERBERTSSON, A.: Dynamic Hedging of Portfolio Credit Risk in a Markov Copula Model. *Journal of Optimization Theory and Applications*, DOI 10.1007/s10957-013-0318-4 (forthcoming).
- [6] BIELECKI, T.R., COUSIN, A., CRÉPEY, S., HERBERTSSON, A.: A bottom-up dynamic model of portfolio credit risk - Part I: Markov copula perspective. Forthcoming in *Recent Advances in Financial Engineering 2012*, World Scientific (preprint version available at <http://dx.doi.org/10.2139/ssrn.1844574>).
- [7] BIELECKI, T.R., COUSIN, A., CRÉPEY, S., HERBERTSSON, A.: A bottom-up dynamic model of portfolio credit risk - Part II: Common-shock interpretation, calibration and hedging issues. Forthcoming in *Recent Advances in Financial Engineering 2012*, World Scientific (preprint version available at <http://dx.doi.org/10.2139/ssrn.2245130>).
- [8] BIELECKI, T. R. AND CRÉPEY, S.: Dynamic Hedging of Counterparty Exposure. Forthcoming in *The Musiela Festschrift*, Zariphopoulou, T., Rutkowski, M. and Kabanov, Y., eds, Springer, 2012.
- [9] BIELECKI, T.R., CRÉPEY, S., JEANBLANC, M.: Up and down credit risk. *Quantitative Finance* 10 (10), pp. 1137–1151 (2010).
- [10] BIELECKI, T.R., CRÉPEY, S., JEANBLANC, M. AND ZARGARI, B.: Valuation and Hedging of CDS Counterparty Exposure in a Markov Copula Model. *International Journal of Theoretical and Applied Finance*, 15 (1) 1250004, 2012.
- [11] BIELECKI, T. R. AND JAKUBOWSKI, J. AND NIEWĘGŁOWSKI, M.: Dynamic Modeling of Dependence in Finance via Copulae Between Stochastic Processes, *Copula Theory and Its Applications*, Lecture Notes in Statistics, Vol.198, Part 1, 33–76, 2010.
- [12] BIELECKI, T.R., VIDOZZI, A. AND VIDOZZI, L.: A Markov Copulae Approach to Pricing and Hedging of Credit Index Derivatives and Ratings Triggered Step-Up Bonds, *J. of Credit Risk*, March 2008.
- [13] BRIGO, D. AND ALFONSI, A: Credit default swap calibration and derivatives pricing with the SSRD stochastic intensity model *Finance and Stochastics*, 9 (1), 29–42, 2005.
- [14] BRIGO, D. AND EL-BACHIR, N.: An Exact Formula for Default Swaptions’ Pricing in the SSRJD Stochastic Intensity Model *Mathematical Finance*, 20 (3), 365-382, 2010.
- [15] BRIGO D., MORINI M. AND PALLAVICINI, A.: *Counterparty Credit Risk, Collateral and Funding with pricing cases for all asset classes*. Wiley, 2013.
- [16] BRIGO, D., PALLAVICINI, A. AND PAPTAEODOROU, V.: Arbitrage-free valuation of bilateral counterparty risk for interest-rate products: impact of volatilities and correlations *International Journal of Theoretical and Applied Finance*, 14 (6), 773–802, 2011.
- [17] BRIGO, D., PALLAVICINI, A., TORRESETTI, R. Credit models and the crisis: default cluster dynamics and the generalized Poisson loss model, *Journal of Credit Risk*, **6**(4), 39–81, 2010.

- [18] BRIGO, D., PALLAVICINI, A., TORRESETTI, R.: Calibration of CDO Tranches with the dynamical Generalized-Poisson Loss model. *Risk Magazine*, May 2007.
- [19] BRIGO, D., PALLAVICINI, A., TORRESETTI, R. Cluster-based extension of the generalized poisson loss dynamics and consistency with single names. *International Journal of Theoretical and Applied Finance*, 10 (4) 607–632, 2007.
- [20] CRÉPEY, S., GRBAC, Z. AND NGUYEN, H. N.: A multiple-curve HJM model of interbank risk. *Mathematics and Financial Economics*, Vol 6, Issue 6, p. 155-190, 2012.
- [21] CRÉPEY, S. AND RAHAL, A.: Simulation/Regression Pricing Schemes for CVA Computations on CDO Tranches, *Communications in Statistics – Theory and Methods* (forthcoming).
- [22] DUFFIE, D. AND GÂRLEANU, N.: Risk and the valuation of collateralized debt obligations, *Financial Analysts Journal*, 57, 41-62, 2001.
- [23] ELOUERKHAOUI, Y.: Pricing and Hedging in a Dynamic Credit Model. *International Journal of Theoretical and Applied Finance*, Vol. 10, Issue 4, 703–731, 2007.
- [24] GLASSERMAN, P.: *Monte Carlo methods in financial engineering*, Springer, 2004.
- [25] HERBERTSSON, A.: Pricing synthetic CDO tranches in a model with Default Contagion using the Matrix-Analytic approach, *The Journal of Credit Risk* 4 (4), 3–35, 2008.
- [26] ISCOE, I., JACKSON, K., KREININ, A. AND MA, X.: An Exponential Approximation to the Hockey Stick Function. *Working Paper, Department of Computer Science, University of Toronto*, 2010.
- [27] ISCOE, I., JACKSON, K., KREININ, A. AND MA, X.: Pricing Synthetic CDOs based on Exponential Approximations to the Payoff Function. *Journal of Computational Finance* 16 (3), 127–150, 2013.
- [28] SCHLÖGL, E. AND SCHLÖGL, L.: A tractable Term Structure Model with Endogenous Interpolation and Positive Interest Rates *Source: Insurance: Mathematics and Economics*, 20 (2), 55–156, 1997.